

# On some aspects of the impact of GPSRO observations in global numerical weather prediction

Massimo Bonavita

Research Department

To be submitted for publication in  
Quart. J. Roy. Meteor. Soc.

May 2013

This paper has not been published and should be regarded as an Internal Report from ECMWF.  
Permission to quote from it should be obtained from the ECMWF.



European Centre for Medium-Range Weather Forecasts  
Europäisches Zentrum für mittelfristige Wettervorhersage  
Centre européen pour les prévisions météorologiques à moyen

Series: ECMWF Technical Memoranda

A full list of ECMWF Publications can be found on our web site under:

<http://www.ecmwf.int/publications/>

Contact: [library@ecmwf.int](mailto:library@ecmwf.int)

© Copyright 2013

European Centre for Medium Range Weather Forecasts  
Shinfield Park, Reading, Berkshire RG2 9AX, England

Literary and scientific copyrights belong to ECMWF and are reserved in all countries. This publication is not to be reprinted or translated in whole or in part without the written permission of the Director. Appropriate non-commercial use will normally be granted under the condition that reference is made to ECMWF.

The information within this publication is given in good faith and considered to be true, but ECMWF accepts no liability for error, omission and for loss or damage arising from its use.

## Abstract

The impact of GPSRO observations on global Numerical Weather Prediction has been analysed with a recent version of the ECMWF Integrated Forecasting System. As in previous studies, the use of GPSRO was found to improve the NWP forecast skill and to drastically decrease model induced temperature biases in the analysis. The maximum forecast impact is in the middle and lower stratosphere, where the GPSRO observations have the smallest errors, but it is also visible in the troposphere. The tropospheric impact of GPSRO comes in part from direct tropospheric measurements and in part from stratosphere-troposphere interactions: This second mechanism is found to be particularly important during the northern hemisphere winter.

The NWP forecast impact of GPSRO observations is compared with that of conventional (ATOVS) and hyperspectral satellite nadir sounders. It is found that while GPSRO data have a smaller impact than those of either class of nadir sounders, they are still able to account for a considerable fraction (30% to 70%) of the global forecast error reduction afforded by the use of the full observing system over a system which only uses conventional observations. When forecast verification is performed against radiosonde observations, GPSRO is found to be the most valuable satellite observing system in the lower stratosphere. This is remarkable in view of the relative sparseness of the GPSRO spatial and temporal coverage and an indication of the potential improvements that a denser GPSRO observing network would be able to provide.

## 1 Introduction

Since the COSMIC (Constellation Observing System for Meteorology, Ionosphere and Climate; Anthes *et al.*, 2000) constellation of Global Positioning System (GPS) receivers started providing GPS radio occultation (GPSRO) measurements in July 2006, GPSRO observations have become an important component of the global observing system used in operational numerical weather prediction (NWP; Healy, 2008; Rennie, 2010; Poli *et al.* 2009; Cucurull, 2010).

The importance of GPSRO observations in operational NWP stems from the fact that they provide all-weather, globally distributed measurements of high accuracy and relatively high vertical resolution with respect to satellite radiances from nadir sounders (Kursinski *et al.*, 1997). In this sense they can deliver complementary information to that available from satellite radiances (Collard and Healy, 2003). Another important feature is that GPSRO observations have very low systematic errors (<0.2 K; Eyre, 2008). This allows GPSRO observations to be assimilated without bias correction, which makes them useful as anchor points for the bias correction algorithms that are commonly applied to satellite radiance observations (Bauer *et al.*, 2013; Dee, 2005).

Despite the numerous research missions and missions of opportunity (CHAMP; GRACE-A, TerraSAR-X, SAC-C; Wickert *et al.* 2005, Wickert *et al.* 2008; ROSA, Perona *et al.*, 2010), GPSRO observations in NWP have only started playing a significant role in operational NWP with the successful assimilation of CHAMP GPSRO measurements at ECMWF (Healy and Thépaut, 2006) and, later, with the introduction of the COSMIC constellation of six satellites. This was due to the near real time availability of observations from CHAMP and COSMIC and of the relatively large number of occultations (2200 per day at peak) which the COSMIC fleet provided. However the end of the CHAMP mission and the aging of the COSMIC fleet mean that the number of occultations available at the time of writing has considerably reduced.

More recently (April 2008) the GRAS GPSRO instrument on board the METOP-A polar orbiter has become operational, thus increasing the number of available GPSRO profiles by around 700 per day. This dataset is expected to be complemented by the companion GRAS instrument on board the METOP-B polar orbiter, launched in September 2012.

It is important to notice that the GRAS receiver is the only fully operational GPSRO instrument currently available. This implies that, for the foreseeable future, the number of near real time GPSRO observations available for operational NWP applications will tend to decrease over time. Since the evolution and continuation of other important components of the satellite-based global observing network are coming under increased scrutiny due to budgetary constraints (see McNally, 2012, for an analysis of the possible repercussions of the degradation of the polar orbiters fleet), it is of interest to re-evaluate the impact of GPSRO data on current operational global NWP.

A variety of authors have reported positive impact of GPSRO data on forecast and analysis quality (Healy, 2013; Radnoty et al. 2010; Rennie, 2010; Cucurull, 2010; Poli et al. 2009; Healy, 2008). However the redundancy of the current global observing system makes it difficult to demonstrate the impact of a single component of the observing network by data denial Observing System Experiments (OSE) with respect to the full observing system. This is especially true at short forecast ranges where the control experiment usually has similar skill and highly correlated errors with the experimental setup, making the choice of the verifying analysis difficult and the interpretation of results not straightforward (Bauer *et al.*, 2013). Furthermore, the complex interactions that can arise among the different components of the Global Observing System (GOS), their systematic errors, the bias correction algorithms and the model biases can make it difficult to disentangle the impact of a single component of the GOS and the relevant physical mechanisms (Healy, 2013). For these reasons we have examined the impact of adding the dataset of GPSRO observations used in operations at ECMWF to a simplified baseline observing system composed of conventional observations and atmospheric motion winds (AMV) from geostationary satellites (Section 2). This is a similar experimental setup to the one used in the OSEs performed by Kelly and Thépaut, 2006, to evaluate the space component of the GOS. We assume here that the impact of the observing system under study over the baseline system will provide an amplified indication of the impact on the full observing system, as long as the new observations do not introduce significant systematic errors in the analysis (Daley, 1991). It is worth stressing, also, that while a baseline system with only conventional observations, even with the addition of AMVs, is a poor proxy for the full system in the southern hemisphere and the tropics, it is on the other hand a skilful assimilation and forecast system for the northern extra-tropics, with only a 12 hour degradation in predictive skill with respect to the full system (Bonavita, 2012). The impact of adding GPSRO observations has been evaluated in terms of analysis and forecast statistical skill scores and in terms of changes to the analysed and forecast mean state of the atmosphere (Section 3). From this analysis an interesting mechanism for the evolution of forecast errors connected to the diagnosis of the polar winter stratospheric vortex has been highlighted.

A complementary way to look at the impact of GPSRO observations is to compare it to that of the two other main sources of temperature sounding information from satellites: The “conventional sounders”, i.e. the sounding instruments of the Advanced TIROS Operational Vertical Sounder (ATOVS) system (AMSU-A, HIRS, MHS); and the “advanced sounders”, i.e., the hyperspectral infrared sounders AIRS

and IASI (Section 4). The relative improvement of forecast skill afforded by each observing system with respect to the baseline observing system is evaluated with respect to ECMWF operational analysis and radiosonde observations. This analysis shows, among other things, that despite the relative scarcity of GPSRO observations with respect to the other satellite sounders, GPSRO has the largest impact in the analysis of temperature in the lower stratosphere.

A summary of the main findings is presented in section 5.

## 2 Experimental Setup

The assimilation and forecast experiments reported here have been performed using version CY38R1 of the ECMWF Integrated Forecasting System (IFS). The analyses are produced with the ECMWF incremental 4D-Var system with two outer loops (inner loop minimizations at T95 and T159 resolution, outer loop at T159 resolution). The 4D-Var assimilation window is 12 hours. The IFS forecast model is run at T159 resolution ( $\approx 125$  km grid spacing) with 91 vertical levels (up to 0.01hPa). While the horizontal resolution is coarser than the current operational resolution (T1279,  $\approx 16$  km grid spacing), we do not believe this affects the validity of our conclusions in any significant way. The satellite observing systems under study have, in fact, broad weighting functions, either in the horizontal (GPSRO) or in the vertical (nadir sounding instruments), which, combined with the characteristics of the structure functions currently used in the IFS 4DVar, tend to produce large scale, smooth analysis increments. Besides, lower resolution has allowed running the experiments over longer periods than would otherwise have been possible.

The assimilation experiments have been run over a winter period (1 January 2011 - 28 February 2011) and a summer period (1 July 2011 - 10 September 2011).

The baseline observing system comprises all operationally available conventional observations and AMVs from geostationary and polar orbiting satellites. The number of observations assimilated in each 12 hour 4D-Var window is of the order of  $6E5$ . During the winter assimilation experiment, bending angles from METOP-A GRAS and COSMIC 1,2,4,5,6 instruments were available. The number of additional observations in a 12 hour window is in the  $1.4E5$ - $1.95E5$  range, corresponding to approx. 800-1100 profiles between 0 and 50 km. In the summer experiment bending angles from METOP-A GRAS, GRACE-A, TerraSAR-X and COSMIC 1,2,4,5,6 were available, providing  $1.7E5$ - $2.2E5$  additional observations in each 12 hour window (approx. 950-1200 profiles). An example of the data coverage provided by the available GPSRO observations over a 12 hour analysis window during the winter experiment is shown in Fig. 1.

In all the experiments presented here the IFS operational background error covariance estimates have been used. This was found to be sub-optimal when running observing system experiments with a much degraded observational coverage with respect to the operational one (McNally *et al.*, 2013). However, the relative difference in observation counts between the baseline and GPSRO experiments with respect to the total number of operationally assimilated observations is less than 2%. This implies that, for the purpose of comparing the relative performance of the baseline and GPSRO systems, the use of specifically tuned background error covariance estimates is likely to be immaterial. On the other hand,

when comparing the performance of the baseline and GPSRO experiments with experiments that use the full operational observing system or a close proxy, then the experimental setup used here can lead to an underestimate of their performance.

The forward model/observation error model for GPSRO observations is the one used operationally at ECMWF (Healy, 2008). It assumes an error standard deviation of 20% of the observed value at 0 km impact height. This error is linearly reduced to 1% of the observed value at 10 km impact height and is kept at this constant relative level above. An absolute minimum value of 3  $\mu$ rad is imposed on the observation error standard deviations in order to control the ionospheric signal, which is thought to be dominated by observation errors (Healy and Thépaut, 2006). Observations errors are assumed uncorrelated. Fig.2 shows the assumed observation error standard deviation profile for GPSRO bending angles (continuous line) and its estimate (dashed line) according to the methodology of Desroziers *et al.*, 2005. This estimated observation error profile has been constructed by gathering background and analysis departures at GPSRO observation locations over a 30 day period during the winter time experiment. While it is difficult in general to give precise estimates of the correct observation errors for most observation types, we can see that the error model used at ECMWF provides estimates which are generally consistent from the point of view of linear estimation theory. Possible exceptions are in the middle to high stratosphere, where current assumed observation errors appear slightly overestimated, and, similarly in the troposphere.

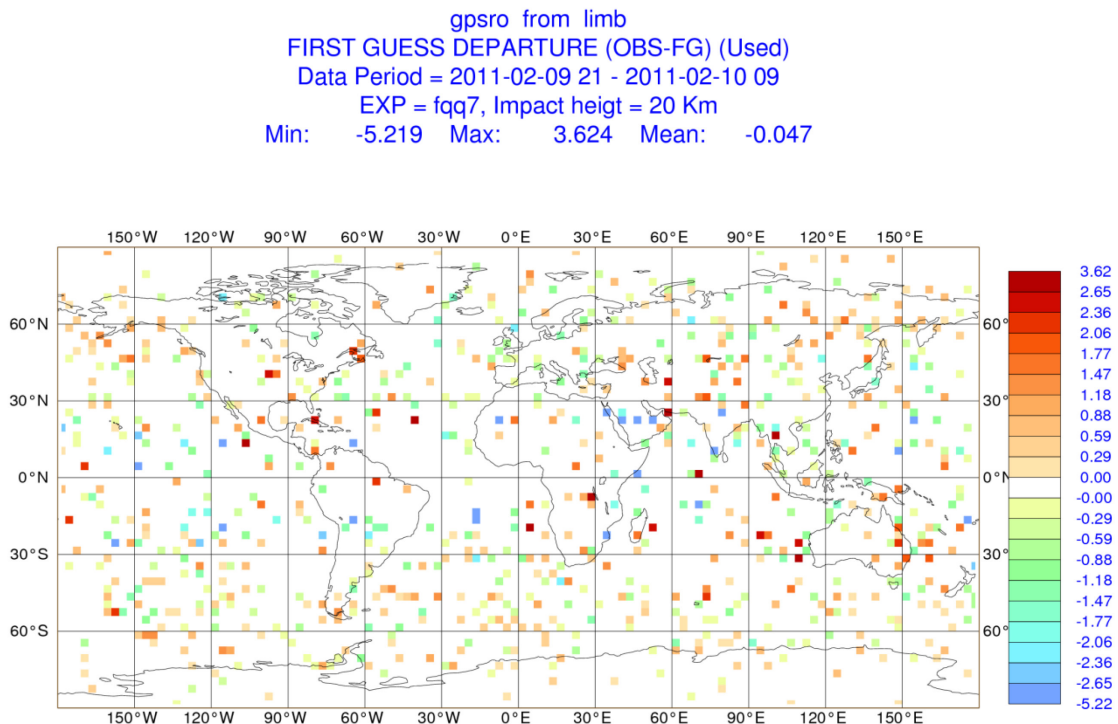


Figure 1: First guess departures of GPSRO bending angles at 20 km impact height assimilated in the 2011/02/10 00UTC analysis of experiment GPS. Units:  $10^{-6}$  radians.

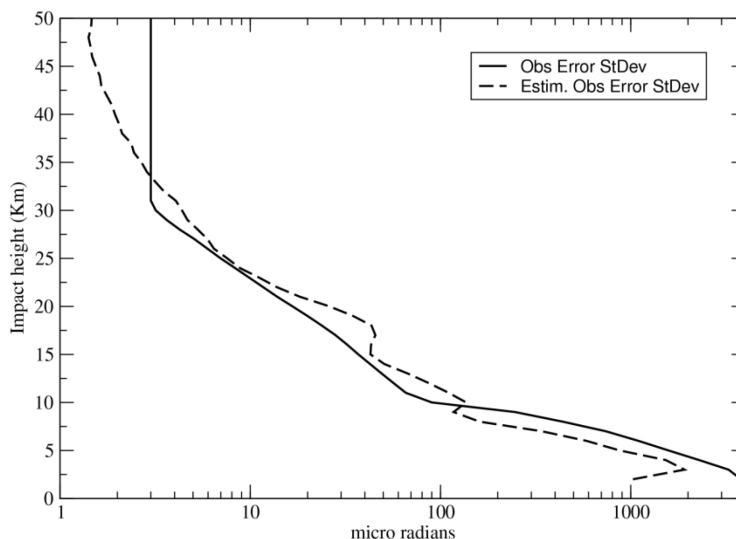


Figure 2: Assumed (continuous line) and estimated (dashed) observation error standard deviations for GPSRO bending angles as a function of impact height. Units:  $10^{-6}$  radians.

### 3 Assimilation experiments: Impact over Baseline System

We analyse here the impact of the use of GPSRO observations on the characteristics and quality of the resulting analysis and forecasts. The control experiment (indicated hereafter as BASE) uses the baseline observing system described in Sec. 2, while the experiment indicated hereafter as GPS makes use of the BASE observations plus all the available GPSRO observations as detailed in Sec.2.

#### a) Impact on Analysis

Fig. 3 presents a zonal average plot of the standard deviation of the temperature difference between the GPS and BASE experiments' analysis. The left panel refers to the winter period, the right to the summer period. As expected, the bulk of the impact on the temperature analysis is in the stratosphere (above 200 hPa), with the exception of the southern extra-tropics, where a considerable impact can also be seen in the troposphere. This is to be expected, as the number of tropospheric profiles from conventional observations (radiosondes + aircraft reports) in the southern extra-tropics (SH) is around 5% of the number available in the northern extra-tropics (NH). Another notable feature of Fig. 3 is that the stratospheric differences are considerably larger in the winter hemispheres. In the northern hemisphere the relative maximum is in the 70N-90N latitude band, suggesting the importance of GPSRO data in the analysis of the polar vortex, due to the relative scarcity of sounding data north of 70N. In the southern hemisphere the relative maximum difference is shifted towards the equator, in the 40S-60S latitude band: This feature reflects both the more symmetric and persistent structure of the Antarctic polar vortex, and the relative scarcity of sounding observations in the southern extra-tropical storm track.

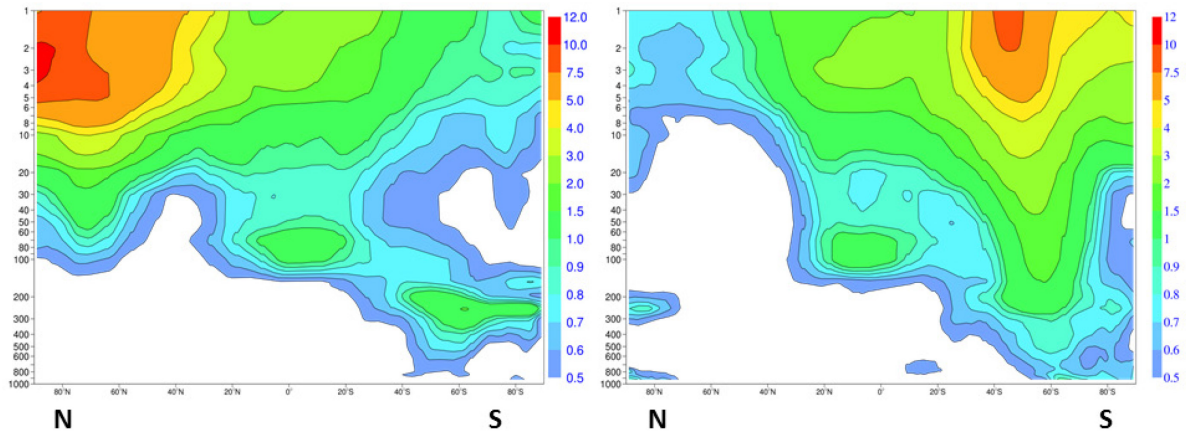


Figure 3: Zonal average of the standard deviation of the difference of the temperature analysis fields between experiments BASE and GPS for the winter period (left panel) and summer period (right panel). Vertical coordinates in hPa; legend in K.

The zonal average of the mean temperature analysis difference (GPS minus BASE) is shown on the first row of Fig. 4. The use of GPSRO tends to correct known IFS model biases (Radnoti *et al.*, 2010), i.e. a small warm bias in the upper troposphere, a cold bias in the lower stratosphere and a warm bias in the medium and upper stratosphere. The impact on the mean zonal wind circulation (Fig. 4, second row) is mainly confined to the stratosphere and results in the strengthening of the intensity of the polar night jet.

A complementary way of looking at the impact of GPSRO on the analysed fields is through the background and analysis departures with respect to observations (O-B and O-A, respectively), generated by the analysis-forecast cycle of the GPS and BASE experiments.

In Fig. 5 we present the standard deviation (left column) and mean difference (right column) of the 12 hour forecast fit (background departures, solid) and the analysis fit (analysis departures, dotted) to radiosonde temperature observations for the GPS experiment (black lines) and the BASE experiment (grey lines). The reduction in the standard deviation of the departures confirms the large global, positive impact of the GPSRO data in the stratosphere. This impact extends down to the middle troposphere in the SH.

The impact on the mean departures is even larger. The GPS experiment has drastically smaller temperature biases with respect to radiosonde observations in the stratosphere. This effect is more apparent in the Tropics and in the SH, where the relative small number of available radiosonde profiles are not able to sufficiently constrain the analysis and thus control model error growth. The signs of the departures also agree with the interpretation that the GPSRO data is trying to counteract the effects of the IFS model drift.

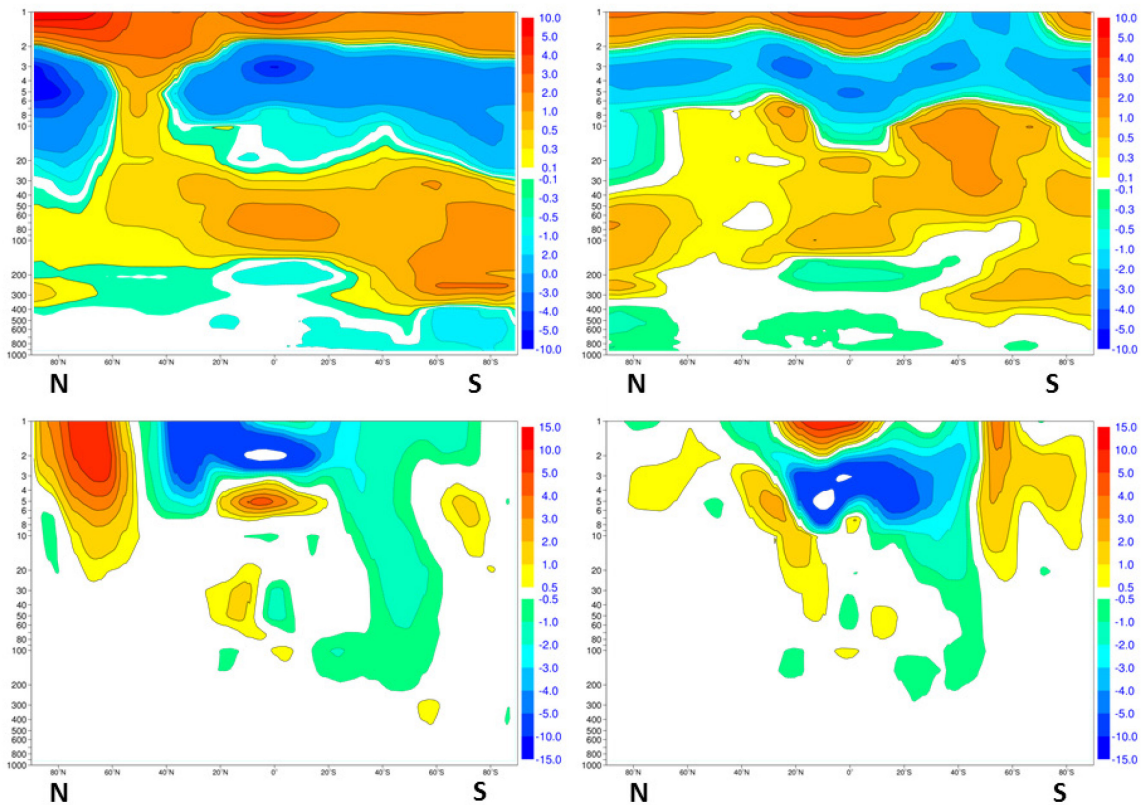


Figure 4: Zonal average of the mean difference of the temperature (first row) and zonal wind (second row) analysis fields between experiments GPS and BASE for the winter period (left column) and summer period (right column). Vertical coordinates in hPa; legends in K for the temperature plots, in m/s for the zonal wind plots.

In Fig. 6 we present the standard deviation (left column) and mean difference (right column) of the 12 hour forecast fit (background departures, solid) and the analysis fit (analysis departures, dotted) to radiosonde zonal wind observations north of 70N. The strong reduction in the mean departures above 20 hPa of the GPS experiment with respect to the base experiment is a clear indication that the introduction of GPSRO observations corrects the model underestimation of the intensity of the stratospheric polar jet.

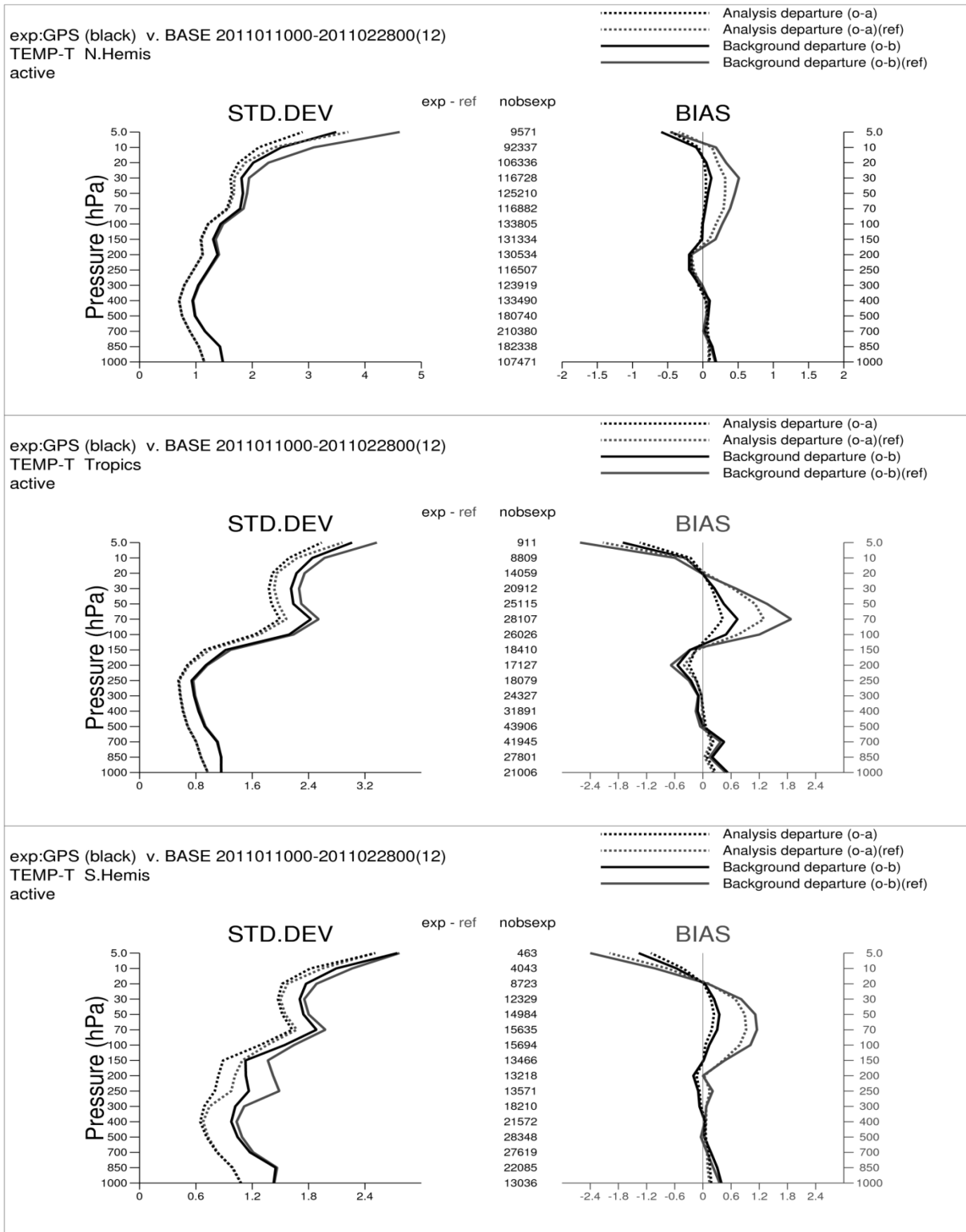


Figure 5: Standard deviation (left column) and mean difference (right column) of the 12 hour forecast fit (background departures, solid) and the analysis fit (analysis departures, dotted) to radiosonde temperature observations for the GPS experiment (black lines) and the BASE experiment (grey lines). First row refers to the northern extra-tropics (90N-20N), second row to the tropics (20N-20S), third row to the southern extra-tropics (20S-90S). Values are averaged over the 2011/01/10 to 2011/02/28 period.

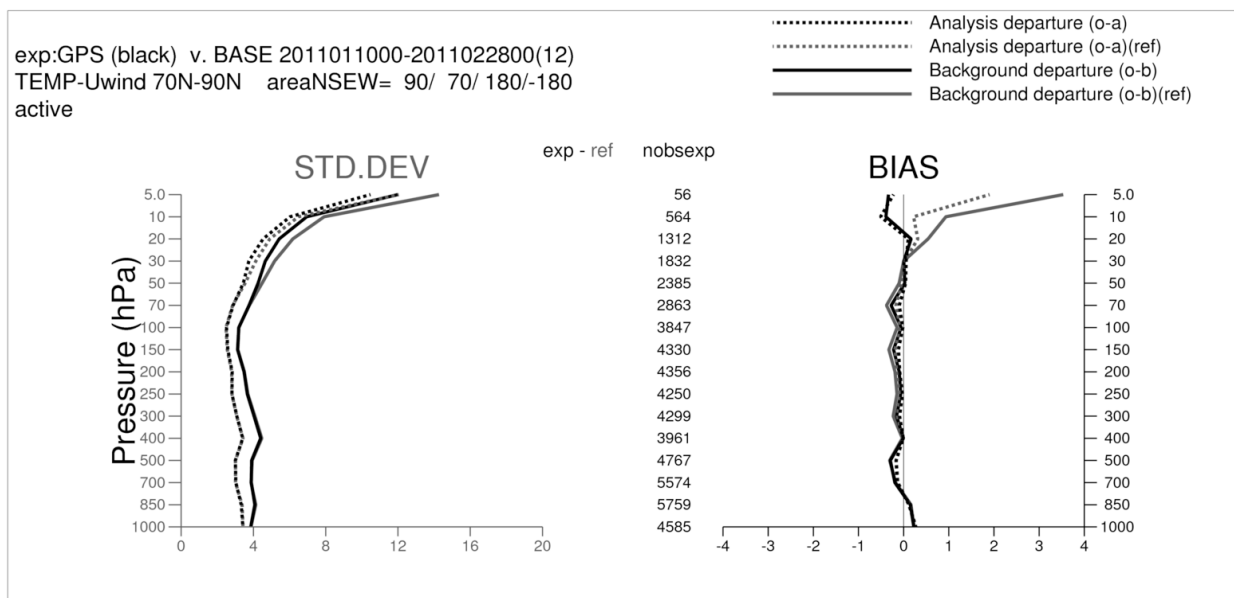


Figure 6: Standard deviation (left column) and mean difference (right column) of the 12 hour forecast fit (background departures, solid) and the analysis fit (analysis departures, dotted) to radiosonde zonal wind observations for the GPS experiment (black lines) and the BASE experiment (grey lines). Radiosondes located north of 70N have been selected. Values are averaged over the 2011/01/10 to 2011/02/28 period.

## b) Impact on Forecast

A first impression of the impact of the additional information from GPSRO data on the forecasts can be obtained from Fig. 7, where the zonal averages of the standard deviation of the difference of the temperature fields between experiments BASE and GPS for the winter period at successive forecast times ( $t+0h$ ,  $t+24h$ , ...,  $t+144h$ ) are plotted.

The impact in the SH analysis (panel (a)) is marked in the middle to higher troposphere and these differences are enhanced in the subsequent forecasts (panels (b) to (f)), extending and intensifying throughout the SH troposphere and lower stratosphere. In the SH the GPSRO data effectively complements the conventional observation network both in the troposphere and in the stratosphere.

In the NH and Tropics, however, the analysis impact is larger at levels approximately above 150 hPa. While in the Tropics the analysis perturbations appear to remain confined to the stratosphere, in the NH they propagate downwards and towards lower latitudes, so that after 5 days most of the NH troposphere is affected. A possible explanation lies with the prevailing NH stratospheric dynamics taking place during the winter experiment.

A commonly occurring NH stratospheric weather pattern during the winter period is shown in Fig. 8. In this weather regime the polar vortex is disrupted and displaced: Enhanced stratospheric cross-polar flow develops (Fig. 8, left column), with strong temperature advection (Fig. 8, right column).

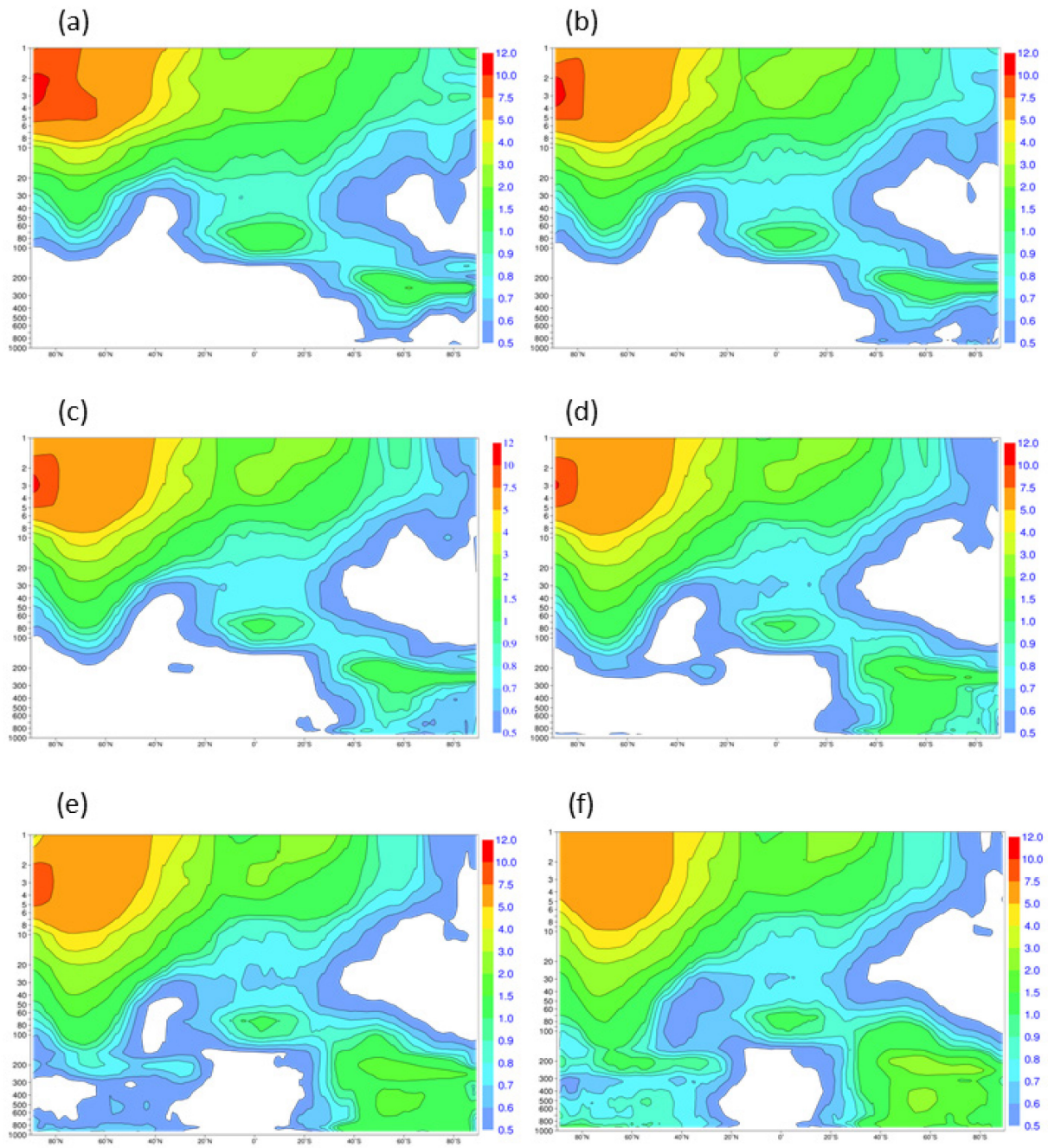


Figure 7: Zonal averages of the standard deviation of the difference of the temperature fields between experiments BASE and GPS for the winter period at forecast time  $t+0h$  (a),  $t+24h$  (b),  $t+48h$  (c),  $t+72h$  (d),  $t+96h$  (e),  $t+120h$  (f). Vertical coordinates in hPa; legend in K.

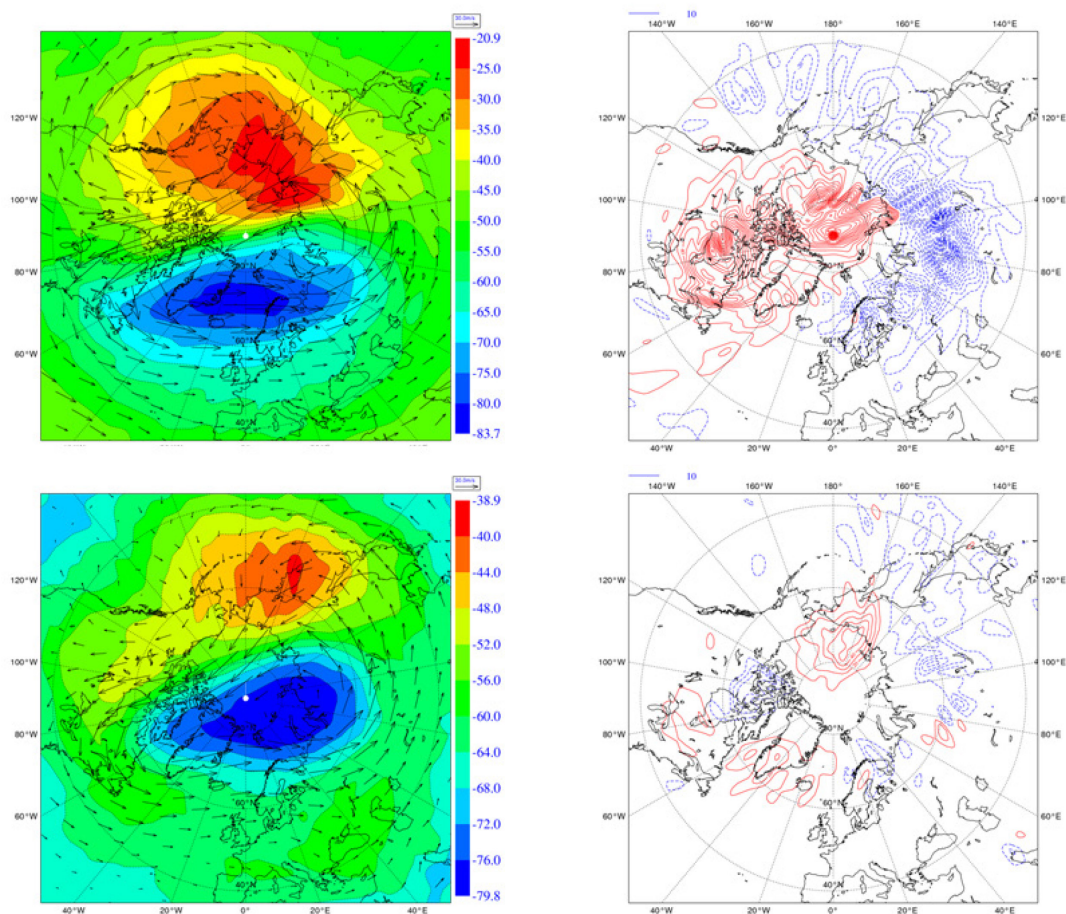


Figure 8: Analysed temperature and wind field (left panels) and temperature advection (right panels) at 10 hPa (upper panels) and 50 hPa (bottom panels) valid on 1 February 2011, 00UTC for the GPS experiment. Isolines of  $10^{-4}$  K/s in the left panels; red contours for positive advection, blue for negative.

The meridional cross section of the wind field shown in Fig. 9 suggests that, in these conditions, differences in the analysis of the stratospheric temperature field can be rapidly advected to lower latitudes and altitudes, resulting in the development of the temperature perturbations shown in Fig. 7. Thus, during the model integration, thermal perturbations develop to produce changes to the meridional temperature gradient and static stability characteristics in the vicinity of the tropopause, which is a well-established mechanism through which the stratosphere circulation interacts with the tropospheric circulation (Simpson *et al.*, 2009 and references therein; Bordi *et al.*, 2009).

This interpretation is confirmed by the forecast skill scores presented in Fig. 10. Here we show the normalised root mean square error reduction of temperature forecasts of experiment GPS with respect to experiment BASE, using the ECMWF operational analysis as verification. As expected the impact is larger in the stratosphere and in SH troposphere. A common feature of these results is that they indicate a larger impact at short verification times which tapers off, but remains statistically significant, at longer lead times. A possible explanation of this feature lies in the fact the GPSRO

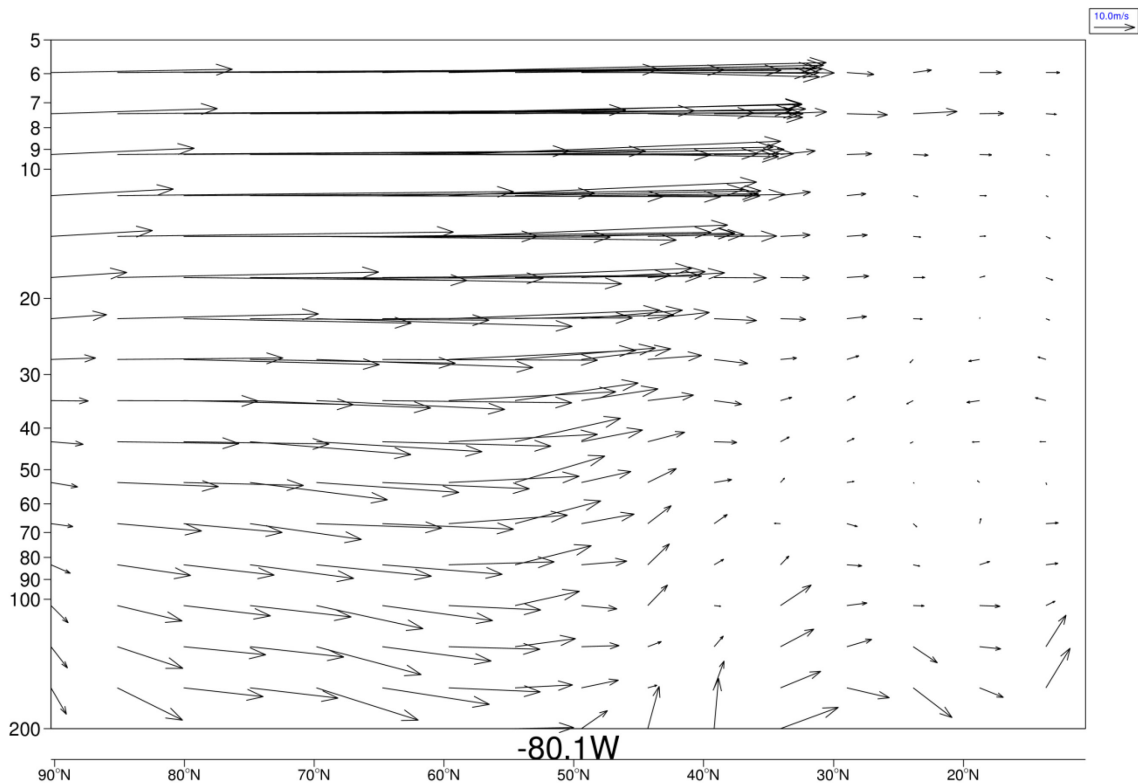


Figure 9: Meridional cross section (5-200 hPa; 90N-10N) of the analysed wind field at 80W longitude valid on 1 February 2011, 00UTC for the GPS experiment. Unit wind arrow is 10m/s.

observation coverage, though fairly homogeneous, is far from being dense enough to completely constrain the analysis, thus reducing its relative impact at longer forecast times. A notable exception to this pattern is however visible in the skill scores for the NH troposphere during the winter experiment (lowest and rightmost three plots). Here we see that the forecast impact of GPSRO stays constant (500 hPa) or even increases (850 and 1000 hPa) with increasing forecast lead time. This confirms that the information from a more accurate stratospheric analysis in the NH winter spreads to the NH tropospheric midlatitudes, in the flow regimes described above. A similar effect is not visible in the SH tropospheric scores of the summer experiment (not shown). This is because of the larger, direct impact of GPSRO on the tropospheric analysis in the SH; and, possibly more importantly, because of the persistent, zonally symmetric character of the Antarctic vortex, which limits cross polar flow and thus tends to keep perturbations more localized.

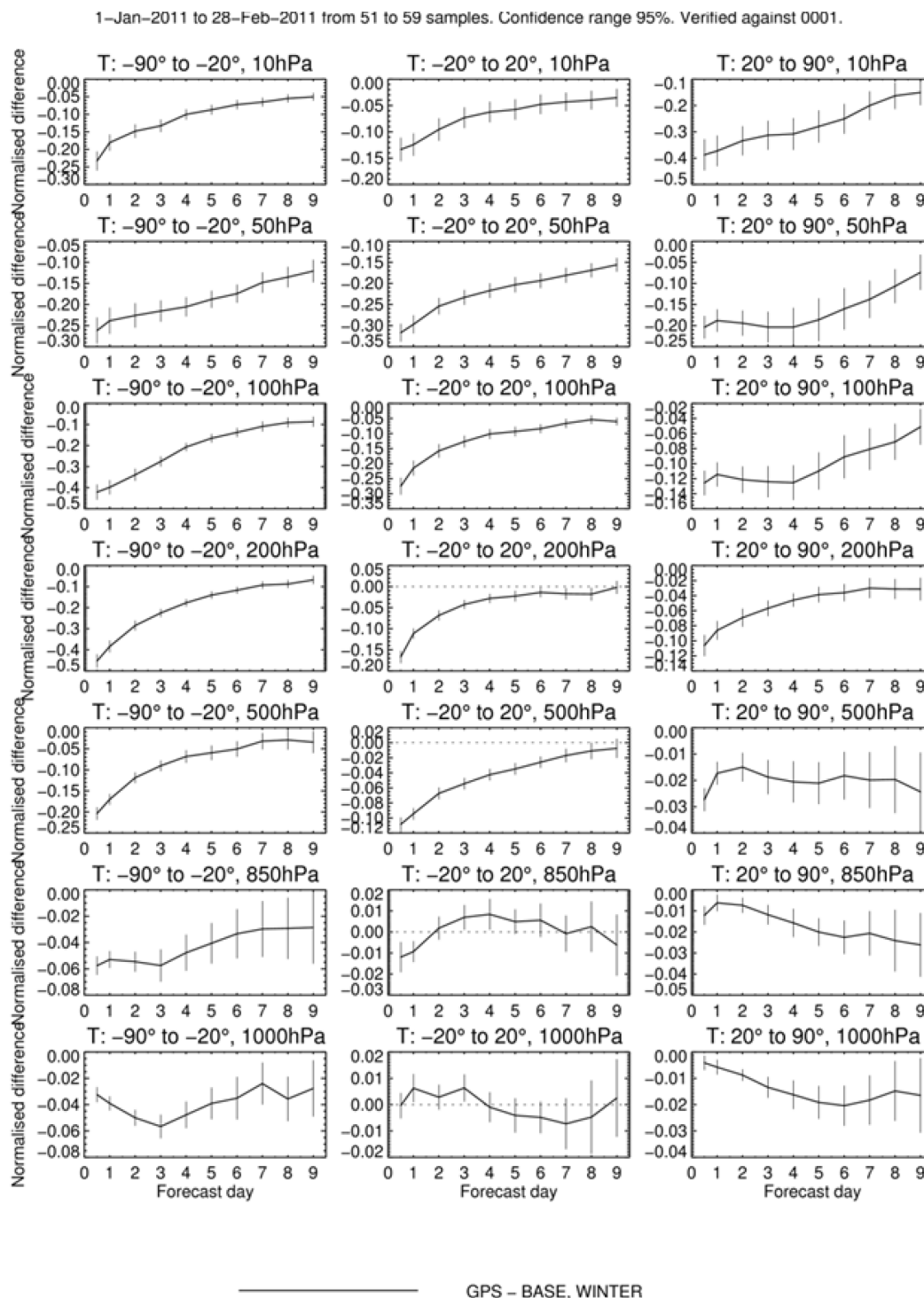


Figure 10: Normalised root mean square error reduction of temperature forecasts of experiment GPS with respect to experiment BASE in the winter period. Reference is the ECMWF operational analysis. The first column refers to the SH, the middle column to the tropics, the right column to the NH. From the top row scores are presented for 10 hPa, 50 hPa, 100 hPa, 200 hPa, 500 hPa, 850 hPa and 1000 hPa (bottom row). Error bars represent 95% confidence levels.

## 4 Assimilation experiments: Relative Impact of Satellite Observing Systems

Another approach to evaluate the impact of GPSRO is to compare its performance relative to the impact of the other main components of the satellite based observing network.

Recent diagnostic work (Cardinali, 2011; Radnoti *et al.*, 2010 and references therein) based on adjoint sensitivity techniques, suggests that the short range (t+24h) forecast error of the IFS is mostly reduced by the AMSU-A (Advanced Microwave Sounding Unit A) temperature sensitive observations (16% relative error reduction), followed by IASI (Infrared Atmospheric Sounding Interferometer) and AIRS (Atmospheric InfraRed Sounder) with 12% each; GPSRO is the third satellite observing system in order of importance, accounting for 6% of the perceived forecast error reduction. Of the other satellite based sensors, scatterometer data account for 5% of error reduction, while AMSU-B, MHS (Microwave Humidity Sounder) and HIRS (High Resolution Infra Red Radiation Sounder) account for 2% to 3%.

Although these estimates are useful for an initial evaluation of the impact of an observing system, they are affected by some limitations: Dependence on the characteristics of the chosen forecast metric; error correlation between the forecast and the verifying state; reliance on the accuracy of the used adjoint operators (see Todling, 2013, for a detailed discussion).

Ultimately, the litmus test of the accuracy of a NWP analysis lies in the accuracy of the forecasts derived from it. Consequently a test of the NWP impact of the GPSRO observing system has been performed relative to the main satellite based sounders. To this end three additional assimilation and forecast experiments have been run.

The first experiment (which we will refer to as “ATOVS”) has been run with the same configuration of the BASE experiment plus the addition of all operationally assimilated observations from the ATOVS (Advanced TIROS Operational Vertical Sounder) package: AMSU-A, AMSU-B/MHS and HIRS. During the experimental periods ATOVS data from NOAA15/18/19, AQUA and METOP-A polar orbiting satellites were available. Restricting our attention to the temperature microwave sounding instrument AMSU-A, which has by far the largest impact in the ATOVS package, the additional observations amount to 110000-120000 profiles for each 12 hour assimilation window (see Fig. 11 for an example of spatial coverage). AMSU-A channels 5 to 14 from all satellites were assimilated (except for channels blacklisted for specific sensor problems (6, 11, 14 for NOAA15; 8 for NOAA19; 5, 7 for AQUA; 7 for METOP-A). These set of microwave channels have broad sensitivity to the atmospheric temperature profile in the 5-50 km height range.

The second experiment (which we will refer to as “HYPER”) has also been run with the same configuration of the BASE experiment plus the addition of the operationally assimilated observations from the two infrared hyperspectral sounders AIRS on board AQUA and IASI on board METOP-A. Even though only a limited subset of available channels from both sounders are used operationally and the number of observations is further reduced by rather stringent data selection and quality control requirements (McNally *et al.*, 2007; Collard and McNally, 2009), the use of both sounders results in

an additional  $\sim 30000$  profiles for each 12 hour assimilation window. In Fig. 12 an example of the spatial coverage afforded by the two hyperspectral sounders over a 12 hour assimilation window is given.

Finally a control experiment (which we will refer to as “CTRL”) with the full observational dataset used in operations at ECMWF was run over the same winter and summer periods. This comprises the BASE+GPSRO+HYPER+ATOVS observations augmented with scatterometer data (ERS and ASCAT) and the use of satellite sounders and imagers (AMSU-A, TMI, SSMIS, AMSR-E) over cloud affected and precipitating areas (Bauer *et al.*, 2010; Geer *et al.*, 2010). The CTRL experiment differs from the operational assimilation and forecast cycle only for the lower resolution of the forecast and the 4DVAR analysis.

As was the case for the BASE and GPS experiments, also the HYPER, ATOVS and CTRL experiments have been run using operational background error statistics in the 4DVar analysis. This is sub-optimal for the HYPER and ATOVS experiments, but the degradation is thought to be smaller than that incurred by the BASE and GPS experiments because the spatial distribution and the observation counts of the observational dataset used in HYPER and ATOVS is much closer (40% and 55% of the total observation number) to the operational one than that of the BASE and GPS experiments (5% and 7% respectively).

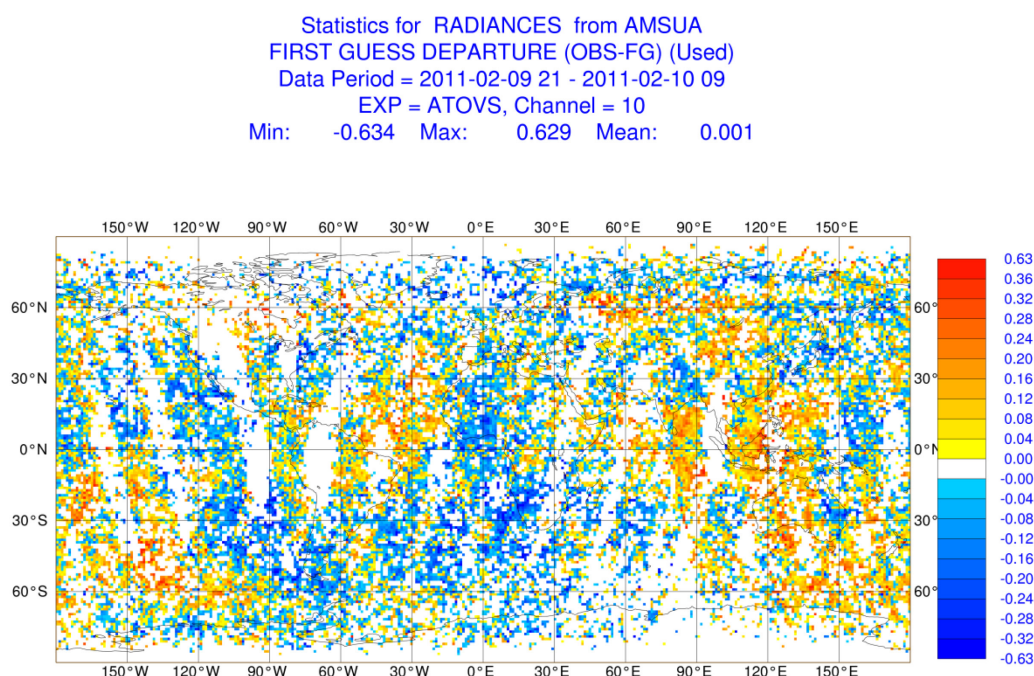


Figure 11: First guess departures of AMSU-A Ch. 10 brightness temperatures from all the available polar orbiters, assimilated in the 2011/02/10 00UTC analysis of experiment ATOVS. Units: K.

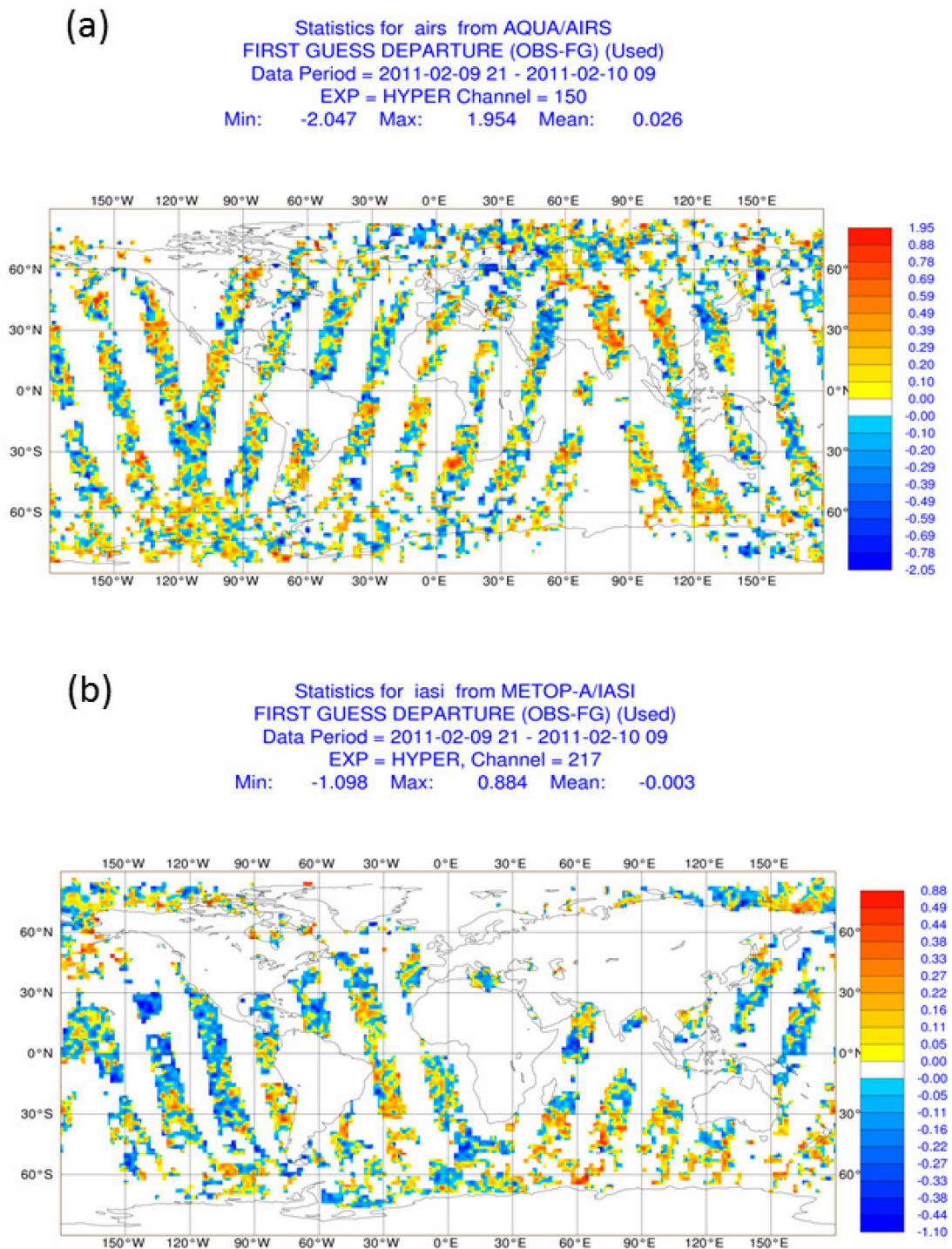


Figure 12: First guess departures of brightness temperatures from AIRS channel 150 on board AQUA (panel (a)) and IASI channel 217 on board METOP-A (panel (b)), assimilated in the 2011/02/10, 00UTC analysis of experiment HYPER. Both are temperature sounding channels with peak sensitivity around 150 hPa. Units: K.

The first row of fig. 13 presents the globally averaged root mean square error profiles of the temperature forecasts valid at t+24h (left), t+72h (middle) and t+120h (right) for experiments BASE and CTRL, computed over the aggregated winter and summer periods. The second row presents the per cent fraction of the (CTRL-BASE) error reduction achieved by experiments GPS (continuous line), HYPER (dashed line) and ATOVS (dash dotted line) at t+24h (left), t+72h (middle) and t+120h (right). It is worth stressing that these results only pertain to the skill of the temperature forecasts. The impact on other quantities such as specific humidity and (for the hyperspectral sounders) ozone which are directly sampled by the nadir sounders are not considered here. Some interesting considerations can be drawn from these results.

Firstly, these plots confirm the pre-eminence in the current IFS configuration of the ATOVS instruments package (and the AMSU-A microwave sounder, in particular) in terms of forecast impact. In the medium range (3 to 5 days), the ATOVS package alone provides 90% or more of the forecast improvement realised by the full operational observing system over the BASE observing system.

The HYPER experiment comes a close second in terms of forecast improvement. In particular, the hyperspectral sounders match the ATOVS performance in the troposphere, and are within 10% of the ATOVS performance in the stratosphere. While there is clearly a large amount of overlapping information coming from the two classes of instruments, which enhances the resilience and robustness of the global observing system, it can still be shown (Radnoti *et al.*, 2010) that the denial of either or both the IASI and AIRS observations leads to a small but significant degradation of scores.

The impact of the GPSRO observations is the smallest of the three classes of sounders considered here, but it is nonetheless very significant. GPSRO can recover from 30% to 70% of the forecast skill improvement generated by the full observing system over the control. This is significant in view of the fact that the number of GPSRO profiles available during the experiments was roughly two orders of magnitude smaller than those of ATOVS and HYPER sounders, and that the use of sub-optimal background error statistics is likely to have impacted on the skill of the GPS experiment in larger measure than on the ATOVS and HYPER experiments

The GPSRO impact can be seen to be largest in the lower stratosphere, where the accuracy of the measurements is assumed to be higher and the observation errors are thus set to relatively smaller values. From the observation error diagnostic presented in Fig. 2, it can be argued that the assumed observation errors could be reduced in the middle to upper stratosphere and, to a lesser extent, in the troposphere. Changing the prescribed observation errors to match more closely their diagnosed values results, in fact, in marginal improvements (not shown) in the quality of the forecast fields, but does not change the overall conclusions.

The plots on the bottom row of Fig. 13 provide some information on the geographical distribution of the GPSRO forecast impact, by showing the per cent fraction of the (CTRL-BASE) error reduction achieved by experiments GPS (continuous line), HYPER (dashed line) and ATOVS (dash dotted line) at t+72h for the northern extra tropics (left panel), the tropics (centre), the southern extra tropics (right). It can be noted how the much denser coverage of conventional observations in the northern hemisphere drastically reduces the tropospheric GPSRO impact (and also the impact of the other

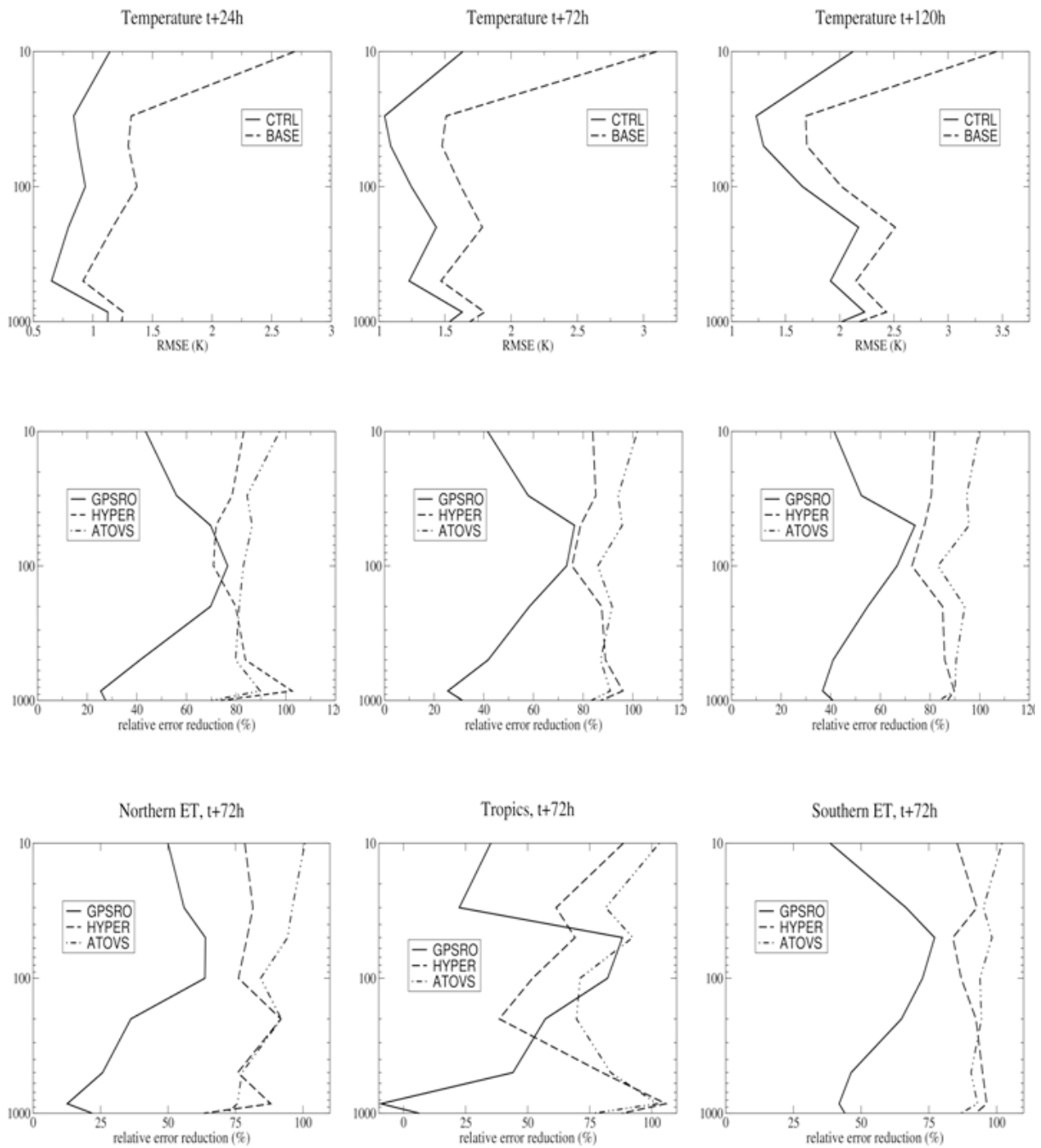


Figure 13: Global RMS error profiles of the temperature forecasts valid at  $t+24h$  (left),  $t+72h$  (middle) and  $t+120h$  (right) for experiments BASE and CTRL (first row; units: K, hPa). The second row presents the per cent fraction of the (CTRL-BASE) error reduction achieved by experiments GPSRO (continuous line), HYPER (dashed line) and ATOVS (dash dotted line) at  $t+24h$  (left),  $t+72h$  (middle) and  $t+120h$  (right). The third row shows the per cent fraction of the (CTRL-BASE) error reduction achieved by experiments GPSRO (continuous line), HYPER (dashed line) and ATOVS (dash dotted line) at  $t+72h$  for the northern extra tropics (left), tropics (centre), southern extra tropics (right). Verification against ECMWF operational analysis.

satellite instruments) with respect to the southern hemisphere. Another interesting aspect is the relatively larger impact of GPSRO in the tropics: here the improvement over the BASE system is comparable to or greater than that of ATOVS and HYPERS in the 50-200 hPa layer but it is also seen to taper off more rapidly in the lower troposphere.

To further investigate this aspect and to filter out the possible influence of the verifying analysis on our results, we have also computed the forecast skill scores with respect to radiosonde observations. An example of the results is given in fig. 14, where we compare the 100 hPa temperature RMS forecast errors computed against the operational ECMWF analysis (left panel) and the radiosonde observations (right panel). The general conclusion is that verification against observations tends to further amplify the impact of GPSRO in the RMS error metric, especially in atmospheric layers where GPSRO impact is already large. This can be understood as ATOVS and HYPERS data make up around 90% of the total assimilated observations and thus have a large influence in changing the mean analysis state. This effect is also visible in Fig. 15, where we show the evolution of the forecast error mean and standard deviation of the BASE, GPS, HYPERS and ATOVS experiments in the tropics, again computed using radiosonde observations as the truth. In the lower stratosphere (50-100 hPa, first two rows in Fig. 15) GPSRO has the largest impact of all satellite components in correcting the model cold bias and also the random component of the forecast error. At 200 hPa (third row of Fig. 15) the model forecast bias changes sign and again GPSRO is the most effective satellite observing system at countering this model drift, while its impact on error standard deviation is comparable to that of the hyperspectral sounders. In the lower troposphere (850 hPa, bottom row in Fig. 15) the model bias changes sign again and it is seen that GPSRO actually increases the systematic error (the impact on error standard deviation being slightly positive). The negative RMSE impact in the lower tropical troposphere, as already noted in Bauer *et al.*, 2013, is thus only due to a change in the analysed mean state caused by the change in sign of the model bias from upper to lower troposphere coupled to the vertical structure of the assumed GPSRO observations errors and the GPSRO observation operator. This effect is also present in the extra-tropics (not shown) but the different density of conventional observations; the different dynamical constraints and the different structure of the background errors (shallower in the extra-tropics) all combine to reduce its impact in the RMSE metric.

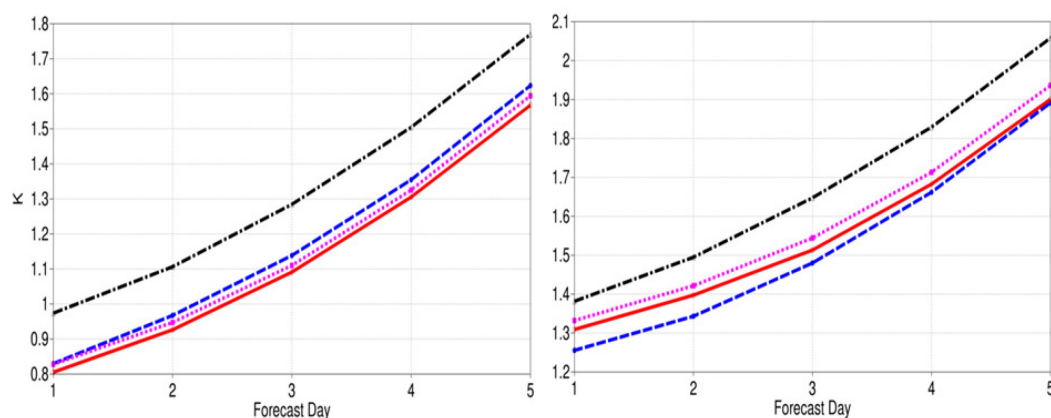


Figure 14: 100 hPa RMS forecast errors in the northern extra-tropics (20N to 90N) for the BASE experiment (dash dot black line), GPSRO (dash blue line), HYPERS (dotted pink line) and ATOVS (continuous red line). Scores are computed with respect to the operational ECMWF analysis (left panel) and to the radiosonde observations (right panel) and are cumulated over the winter and summer periods.

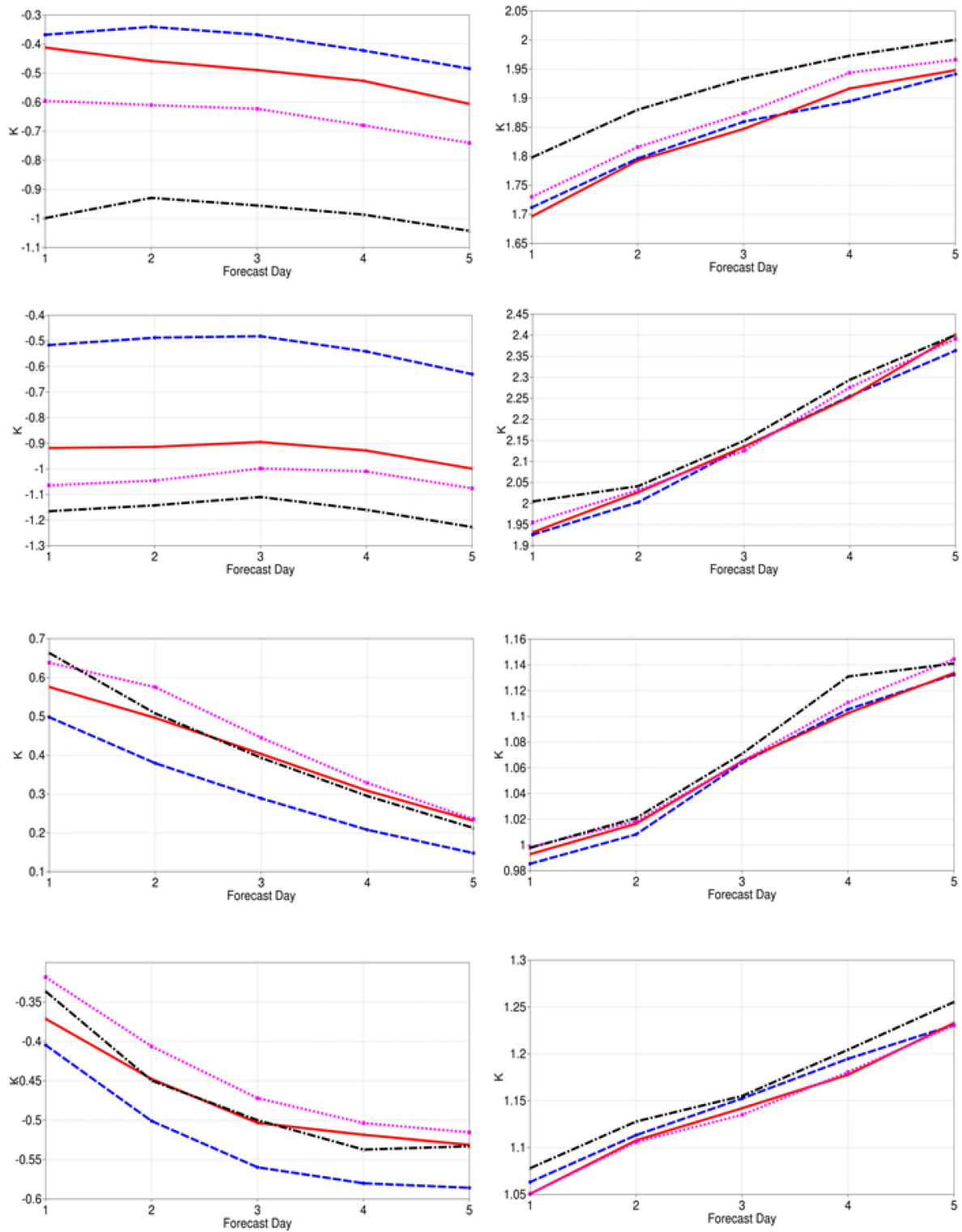


Figure 15: Mean (left column) and standard deviation (right column) of forecast errors in the tropics (20N to 20S) for the BASE experiment (dash dot black line), GPSRO (dash blue line), HYPER (dotted pink line) and ATOVS (continuous red line). First row presents 50hPa scores, second 100 hPa, third 200 hPa, bottom row 850 hPa Scores are computed with respect to radiosonde observations and are cumulated over the winter and summer periods.

## 5 Summary and Conclusions

Over the past few years GPSRO has become a fundamental component of the global observing system used in NWP. This is both because of the beneficial impact of accurate, unbiased GPSRO observations on the accuracy of atmospheric analysis, and because of the indirect impact of GPSRO observations as anchors for the bias correction of radiance observations from nadir sounders.

The impact of GPSRO observations on NWP skill has been examined by running assimilation and forecast experiments with a recent version of the ECMWF IFS. As in earlier studies (Kelly and Thépaut, 2006), this has been done using in the control experiments a degraded, but still skilful, observing system composed of conventional and AMVs observations. In this way the signal generated by adding new observations is easier to distinguish than it would be possible from a simple data denial experiment, given the relatively high degree of redundancy of the current global observing system. As importantly, this framework allows an easier understanding of the mechanisms by which an observation type impacts the analysis and forecasts.

In terms of analysis accuracy, results of the present work confirm the importance of the GPSRO measurements in reducing the effect of model biases in the analysed state in the upper troposphere and the stratosphere. This effect is evident for the temperature field throughout a large part of the atmospheric column and for the wind field in the analysis of the polar night jet.

The impact of GPSRO observations is also apparent in the improved accuracy of the forecasts. In comparison to a much degraded observing system such as the one available in the SH for the control experiment, the GPSRO data consistently improves forecast skill throughout the atmospheric column and forecast ranges. In the NH, on the other hand, the conventional observational coverage is much denser, especially in the troposphere. This results in a smaller impact of the GPSRO data in general and in the tropospheric scores in particular. Interestingly, the positive impact that GPSRO data have on the tropospheric scores in the NH winter appears to be primarily the result of stratospheric-tropospheric interactions: The GPSRO observations change the stratospheric polar temperature analysis and these perturbations propagate equatorward and downward and affect the forecast of the tropospheric flow in the medium range. This effect is present in the NH winter only, and it appears to be related to the disruption of the polar vortex and the associated enhanced cross polar flow.

The influence of GPSRO on NWP forecast skill has also been analysed in terms of its relative impact with respect to the two other main sources of satellite observed temperature profiles (ATOVS and hyperspectral sounders) and to the full observing system. It is found that, on a global basis, GPSRO can recover 30% to 70% of the temperature forecast error reduction of the full observing system with respect to a conventional observing system when verified assuming the ECMWF operational analysis as truth. This is still below the 80% to 90% error reduction that ATOVS and hyperspectral sounders can each separately provide, but it is still remarkable because the number of available GPSRO profiles is roughly two orders of magnitudes smaller than either ATOVS or hyperspectral sounders' counts. Disaggregating the global impact scores for different latitude bands, it is apparent that GPSRO impact is larger in the tropics and in the southern extra tropics, where the density of conventional observations is sparse. The GPSRO forecast impact is also found to be relatively larger when verification is

performed against radiosonde observations. [This is particularly apparent in the lower stratosphere, where the capacity of GPSRO measurements to correct for large temperature model biases makes it the most valuable satellite observing system. The experimental setup on which these results are based is somewhat sub-optimal in terms of spatial resolution and background errors model, as is commonly the case with OSEs. However, the structure of the satellite instruments weighting functions, the structure of the background errors covariances and the expected impact of the satellite instruments observation density and distribution on background errors, give us confidence that our main conclusions will stand for more realistic experimental frameworks.

In conclusion, the results presented in this study confirm the importance of GPSRO measurements in current global NWP and support the case for the continuation and the expansion of the currently available operational GPSRO constellation.

## Acknowledgments

Fruitful discussions with Sean Healy and Jean-Noël Thépaut are gratefully acknowledged. Development work on the assimilation of RO observations at ECMWF is funded by EUMETSAT Radio Occultation Meteorology SAF.

## References

- Anthes, R., Rocken C., Kou Y-H., 2000: Applications of COSMIC to meteorology and climate. *Terrestrial Atmospheric and Oceanic Sciences* **11**:115-156.
- Bauer, P., A. Geer, P. Lopez and D. Salmond, 2010: Direct 4D-Var assimilation of all-sky radiances. Part I: Implementation. *Q. J. R. Meteorol. Soc.*, **136**: 1868–1885.
- Bauer, P., G. Radnoti, S. Healy, and C. Cardinali, 2013: GNSS radio occultation constellation observing system experiments. ECMWF Tech. Memorandum, n. 692. (Available from: <http://www.ecmwf.int/publications/>)
- Bonavita, M., 2012: [Ensemble of data assimilations and uncertainty estimation](#). Proceedings of the ECMWF Seminar on Data Assimilation for atmosphere and ocean, Reading, UK, 6-9 September 2011. (Available from: <http://www.ecmwf.int/publications/>)
- Bonavita, M., L. Isaksen and E. Holm, 2012: On the use of EDA background error variances in the ECMWF 4D-Var, *Q. J. R. Meteorol. Soc.*, **138**: 1540–1559.
- Bordi, I., K. Fraederich, M. Ghil and A. Sutera, 2009: Zonal Flow Regime Changes in a GCM and in a Simple Quasigeostrophic Model: The Role of Stratospheric Dynamics. *J. Atmos. Sci.*, **66**, 1366–1383.

- Cardinali, C., 2011: Monitoring the assimilation and forecast system performance. Presentations of the ECMWF Seminar on Data assimilation for atmosphere and ocean, 6 - 9 September 2011, Reading, UK. (Available from: <http://www.ecmwf.int/publications/>)
- Collard, A., Healy, S., 2003: The combined impact of future space-based atmospheric sounding instruments on numerical weather prediction analysis fields: a simulation study. *Q. J. R. Meteorol. Soc.*, **129**: 2741–2760.
- Cucurull L., 2010: Improvement in the Use of an Operational Constellation of GPS radio occultation Receivers in Weather Forecasting. *Wea. Forecasting* **25**: 749-767.
- Collard, A. D. and A. P. McNally, 2009: The assimilation of Infrared Atmospheric Sounding Interferometer radiances at ECMWF. *Q. J. R. Meteorol. Soc.* **135**: 1044–1058
- Daley, R., 1991: Atmospheric Data Analysis. Cambridge Univ. Press, 457 pp.
- Desroziers, G., L. Berre, B. Chapnik and P. Poli, 2005: Diagnosis of observation, background and analysis-error statistics in observation space. *Q. J. R. Meteorol. Soc.*, **131**, 3385–3396.
- Eyre, M., 2008: An Introduction to GPS Radio Occultation and its use in numerical weather prediction. Proceedings of the ECMWF GRAS SAF Workshop on Applications of GPS Radio Occultation Measurements, 16 - 18 June 2008, ECMWF, pages 1–10.(Available from: <http://www.ecmwf.int/publications/>)
- Geer, A., P. Bauer, P. Lopez and D. Salmond, 2010: Direct 4D-Var assimilation of all-sky radiances. Part II: Assessment. *Q. J. R. Meteorol. Soc.*, **136**: 1886–1905.
- Healy S. B., 2008: Forecast impact experiment with a constellation of GPS radio occultation receivers. *Atmos. Sci. Let.* **9**:111-118.
- Healy, S. B. (2013): Surface pressure information retrieved from GPS radio occultation measurements. *Q.J.R. Meteorol. Soc.*.. doi: 10.1002/qj.2090
- Healy, S. B. and J.-N. Thépaut (2006): Assimilation experiments with CHAMP GPS radio occultation measurements. *Q.J.R. Meteorol. Soc.* **132**, 605-623.
- Kelly, G. and J.-N. Thépaut (2006): Evaluation of the impact of the space component of the Global Observing System through Observing System Experiments. EUMETSAT/ECMWF Fellowship Programme Research Report (Final Report SOW EUM.MET.SOW.04.0290). (Available from: <http://www.ecmwf.int/publications/>)
- Kursinski, E. R., G. A. Hajj, K. R. Hardy, J. T. Schofield and R. Linfield, 1997: Observing Earth's atmosphere with radio occultation measurements. *J. Geophys. Res.*, **102**: 23429-23465.

- Isaksen, L., M. Bonavita, R. Buizza, M. Fisher, J. Haseler, M. Leutbecher and Laure Raynaud, 2010: Ensemble of data assimilations at ECMWF. ECMWF Tech. Memorandum, n. 636. (Available from: <http://www.ecmwf.int/publications/>)
- McNally, A.P., P. D. Watts, J. A. Smith, R. Engelen, G. A. Kelly, J. N. Thépaut and M. Matricardi, 2006: The assimilation of AIRS radiance data at ECMWF, *Q. J. R. Meteorol. Soc.*, **132**, 935–957.
- McNally, T., 2012: Observing System Experiments to Assess the Impact of Possible Future Degradation of the Global Satellite Observing Network. ECMWF Tech. Memorandum, n. 672. (Available from: <http://www.ecmwf.int/publications/>)
- McNally, T., M. Bonavita and J. N. Thépaut, 2013: The role of satellite data in the forecasting of hurricane Sandy. ECMWF Tech. Memorandum, n. 696. (Available from: <http://www.ecmwf.int/publications/>)
- Perona G., Notarpietro R., Molinaro M., Casotto S., Zoccarato P., Nardo A., Cucca M., Paoletta S., Bordi I., Sutera A., Tartaglione N., Speranza A., Nava B., Radicella S., Vespe F., 2010: The Italian GPS radio occultation experiment on board the Indian satellite Oceansat-2. Proceedings of the 12<sup>th</sup> International Conference on Electromagnetics in Advanced Applications, ICEAA'10, 681-684.
- Poli, P., P. Moll, D. Puech, F. Rabier, and S. B. Healy, 2009: Quality Control, Error Analysis, and Impact Assessment of FORMOSAT-3/COSMIC in Numerical Weather Prediction. *Terr. Atmos. Oceanic Sci.*, 20(1), 101-113.
- Radnòti, G., P. Bauer, A. McNally, C. Cardinali, S. Healy and P. de Rosnay, 2010: ECMWF study on the impact of future developments of the space-based observing system on Numerical Weather Prediction. ECMWF Tech. Memorandum, n. 638. (Available from: <http://www.ecmwf.int/publications/>)
- Rennie, M.P., 2010: The impact of GPS radio occultation assimilation at the Met Office. *Q. J. R. Meteorol. Soc.*, **136**, 116-131.
- Simpson, I. R., M. Blackburn, and J. D. Haigh, 2009: The role of eddies in driving the tropospheric response to stratospheric heating perturbations. *J. Atmos. Sci.*, **66**, 1347–1365.
- Todling, R, 2013: Mon. Wea. Rev., doi: <http://dx.doi.org/10.1175/MWR-D-12-00100.1>.
- Wickert, J., G. Beyerle, R. Koenig, S. Heise, L. Grunwaldt, G. Michalak, Ch. Reigber, T. Schmidt, 2005: GPS radio occultation with CHAMP and GRACE: A first look at a new and promising satellite configuration for global atmospheric sounding, *Annales Geophysicae*, **23**, 653-658.
- Wickert, J., C. Arras, C.O. Ao, G. Beyerle, C. Falck, L. Grunwaldt, S.B. Healy, S. Heise, A. Helm, C.Y. Huang, N. Jakowski, R. Koenig, T. Mannucci, C. Mayer, G. Michalak, P. Poli, M. Rothacher, T. Schmidt, R. Stosius, and B. Tapley, 2008: CHAMP, GRACE, SAC-C, TerraSAR-X/TANDEM-X: Science results, status and future prospects. Proceedings of the ECMWF GRAS SAF Workshop on Applications of GPS Radio Occultation Measurements, 16 - 18 June 2008, ECMWF, pages 43–52. (Available from: <http://www.ecmwf.int/publications/>)

